Basin Research (1992) **4**, 73–90

The large-scale dynamics of grain-size variation in alluvial basins, 1: Theory

Chris Paola*, Paul L. Heller† and Charles L. Angevine†

**Department of Geology and Geophysics, University of Minnesota, Minneapolis, MN 55455; †Department of Geology and Geophysics, University of Wyoming, Laramie WY 82071, USA*

ABSTRACT

We study the interplay of various factors causing vertical grain-size changes in alluvial basins using a simple coupled model for sediment transport and downstream partitioning of grain sizes. The sediment-transport model is based on the linear diffusion equation; by deriving this from first principles we show that the main controls on the diffusivity are water discharge and stream type (braided or single-thread). The grain-size partitioning model is based on the assumption that the deposit is dominated by gravel until all gravel in transport has been exhausted, at which point deposition of the finer fractions begins.

We then examine the response of an alluvial basin to sinusoidal variation in each of four basic governing variables: input sediment flux, subsidence rate, supplied gravel fraction, and diffusivity (controlled mainly by water flux). We find that, except in the case of variable gravel fraction, the form of the basin response depends strongly on the time-scale over which the variation occurs. There is a natural time-scale for any basin, which we call the 'equilibrium time', defined as the square of basin length divided by the diffusivity. We define 'slow' variations in imposed independent variables as those whose period is long compared with the equilibrium time. We find that slow variation in subsidence produces smoothly cyclic gravel-front migration, with progradation during times of low sedimentation rate, while slow variation in sediment flux produces gravel progradation during times of high sedimentation rate. Slow variation in diffusivity produces no effect. Conversely, we define 'rapid' variations as those whose period is short compared with the equilibrium time. Our model results suggest that basins respond strongly to rapid variation in either sediment flux or diffusivity; in both cases, deep proximal unconformities are associated with abrupt gravel progradation. This progradation occurs during times of either low sediment flux or high diffusivity. On the other hand, basin response to variation in subsidence rate gradually diminishes as the time scale becomes short relative to the equilibrium time. Each of the four variables we have considered – input sediment flux, subsidence, gravel fraction, and diffusivity – is associated with a characteristic response pattern. In addition, the time scale of imposed variations relative to the equilibrium time acts in its own right as a fundamental control on the form of the basin response.

1 INTRODUCTION

Changes in grain-size are among the most fundamental and readily observed features of sedimentary sequences. Grain-size is the primary basis on which lithostratigraphic units are defined, and vertical changes in grain-size have long been thought to contain important information about the history of basin sedimentation. The cause of moderate-to-large-scale vertical grain-size variation can be divided into *autocyclic* mechanisms, which originate within the sedimentary system, and *allocyclic* mechanisms, which are externally forced. Broadly speaking, autocyclic effects can be expected to dominate at small to moderate scales and allocyclic effects at large scales, although there is a wide range of overlap in scale.

In this paper we consider allocyclic mechanisms that influence the overall grain-size pattern of alluvial basin fills. One can identify three schools of thought on the origin of allocyclic grain-size variation. In the most traditional school, an increase in grain-size is thought to result from an increase in flux of coarse sediment into the basin during periods of heightened tectonic activity (Rust & Koster

1984). This is often termed 'syntectonic' progradation. A diametrically opposed interpretation was suggested by Blair & Bilodeau (1988) and Heller *et al.* (1988), who argued that periods of tectonic quiescence might be expected to reduce basin subsidence rates and thus allow progradation of coarse units farther into the basin. Thus, to the extent that subsidence is linked to tectonism, upward coarsening would be associated with *reduced* tectonic activity. Gravel progradation in this scenario might be termed 'antitectonic'. Paola (1988, 1990) suggested that either scenario is possible, with the critical control being the variation in sediment flux relative to variation in the rate and distribution of subsidence. The third school (Lindsay, Smith & Haynes 1990; Smith & Battuello 1990) proposes that progradation of coarse material, and thus upward coarsening, can occur because of climatically driven changes in either water or sediment supply, independent of tectonism. Clearly, these three controls – gravel flux, subsidence, and climate – are not mutually exclusive, and any one might dominate in a particular progradation event. The real issue is how to distinguish among them.

We believe that application of well-founded physical models of basin processes can help resolve the roles of these various influences on grain-size patterns in basins. In this paper we develop a simple model of basin filling and grain-size partitioning by rivers, and then look systematically at the effects of varying each of the governing parameters on different time-scales. The model that we develop is first-order and thus does not attempt to replicate all of the important features of real rocks. Despite its simplicity, however, it produces a surprisingly rich set of responses to simple allocyclic forcing. We hope that these idealized response patterns will be helpful in distinguishing among the possible causes of grain-size changes in real rocks. In our companion paper (Heller & Paola 1992; hereafter Part 2) we give examples of how the model can be applied to the interpretation of the rock record.

The basic model is derived directly from the governing equations of flow and sediment transport in rivers. Developing the model from first principles helps clarify what aspects of the fluvial system are and are not embodied in it, and what the model parameters mean physically. This approach also offers the eventual possibility of constraining some of the parameters independently and thus developing truly predictive analytical models in basin analysis.

2 BASIN-FILLING MODEL

2.1 General

Predictive basin-filling models have received increasing emphasis recently (Cross & Harbaugh 1990). A mathematical model provides a framework within which the effects of varying any single factor can be readily determined, and the interaction among variables studied systematically. Such models are also helpful in identifying critical field relations and in guiding the design of field studies. Ultimately, quantitative models are also far more restrictive, and thus far easier to test and refine, than qualitative ones. We note that all of the parameters in our model can, in principle, be estimated independently, offering the possibility that models such as this one may eventually be useful as genuine predictive tools.

The model we develop here begins with simplified forms of the equations of flow and sediment transport in two dimensions. We show that these can be reduced to the linear diffusion equation with two limiting values for the diffusivity, one that we identify with braided streams and the other with single-thread or meandering streams. The diffusion metaphor has long been used in modelling river systems (Adachi & Nakatoh 1969; Garde, Ranga Raju & Mehta 1981; Jain 1981; Soni 1981; Gill 1983; Jaramillo & Jain 1984; Ribberink & van der Sande 1985; Begin 1987; Zhang & Kahawita 1987) and has recently been applied to deltas (Kenyon & Turcotte 1985) and foreland basins (Flemings & Jordan 1989; Jordan & Flemings 1990). Our explicit derivation of the diffusion equation as it applies to basin filling clarifies some of the assumptions implicit in diffusion-based models and allows us to determine the structure of the diffusion coefficient in terms of more fundamental variables. It turns out that the main controls on the diffusion coefficient are the total amount of surface water available in the system, determined by the precipitation rate and the catchment area, and the river type (braided versus single-thread). Overall, four basic independent variables govern the model system: subsidence (rate and distribution), sediment flux, water flux, and grain-size distribution of the sediment supply.

We then couple the diffusional solutions to a simple sediment-partitioning technique for calculating downstream grain-size changes. This technique is based on the observation that in aggrading river systems the primary cause of downstream fining appears to be preferential deposition of the coarsest clasts (Shaw & Kellerhals 1982). This implies that the downstream distribution of grain-size is controlled essentially by mass-balance rather than clast-attrition effects. We exploit this mass-balance control by partitioning the input grain sizes in the deposit according to their proportion in the supply – for instance, if the sediment supply contains 10% gravel and there is no erosion within the basin, gravel will occupy the most proximal 10% of the deposit volume. However, if there is erosion of previously deposited gravel, then this gravel is added to the supply and redistributed farther out into the basin.

As mentioned earlier, this model is not intended to predict the pattern of deposition in a specific basin. Broadly, one can think of the pattern of fill in a given basin as the result of the interplay between specific local effects, such as the geometry of the basin and the distribution of sediment sources, and general patterns of sediment distribution. We hope that our model will help clarify these general patterns, but the local controls can be resolved only through detailed field work.

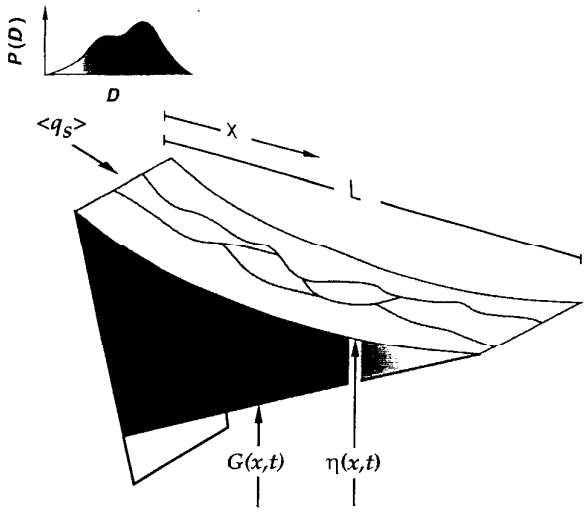

Fig. 1 Definition sketch.

2.2 Modelling sediment distribution

Consider a two-dimensional slice of a sedimentary basin such as shown in Fig. 1. By 'two-dimensional' we mean that the subsidence rate, sediment flux, and water flux do not vary normal to the direction of transport. Conservation of water mass in a single channel can be expressed as

$$Q = bhu, \tag{1}$$

where Q is water discharge $[\Lambda^3\Theta^{-1}]$, b is channel width $[\Lambda]$, h is channel depth $[\Lambda]$, and u is mean velocity $[\Lambda\Theta^{-1}]$. Here and in all subsequent equations the basic units of each variable are given in square brackets: [M = mass, Λ = length, and Θ = time]. The symbol [0] means the variable is non-dimensional. It is more useful to normalize equation (1) to unit basin width, giving

$$q = \beta hu, \tag{2}$$

where q is the normalized water discharge $[\Lambda^2\Theta^{-1}]$ and β the normalized total channel width [0]; both are normalized per unit width of basin.

For sufficiently long space and time-scales, conservation of momentum can be written as

$$\tau = -gh\frac{\partial\eta}{\partial x}, \tag{3}$$

where τ is the kinematic shear stress (force per unit area per unit fluid density) $[\Lambda^2\Theta^{-2}]$, g is gravitational acceleration $[\Lambda\Theta^{-2}]$, η is elevation of the sediment surface relative to a fixed (non-subsiding) horizontal datum $[\Lambda]$, and x is downstream distance $[\Lambda]$. The limiting space and time-scales for which (3) is valid are discussed further in section 2.7.

Conservation of mass for the sediment can be expressed as

$$r = \left(\frac{-1}{C_0}\right)\frac{\partial(\beta q_s)}{\partial x}, \tag{4}$$

where r is the rate of deposition $[\Lambda\Theta^{-1}]$, t is time $[\Theta]$, C_0 is the volume concentration of sediment in the bed [0], and q_s is the volume rate of sediment transport per unit width of channel $[\Lambda^2\Theta^{-1}]$.

There is no explicit relation available for momentum conservation for sediment being transported by a moving fluid. The best one can do is to use a well founded semi-empirical relation (see the review in Brownlie 1981). The simple relation of Meyer-Peter & Müller (1948) can be written as

$$q_s = \frac{8(\tau-\tau_c)^{3/2}}{g(s-1)}, \tag{5}$$

where τ_c is the critical shear stress needed to set the sediment in motion, which for present purposes may be taken as a function of only the local mean sediment grain-size, and s is the sediment specific gravity.

Equations (4) and (5) combine to yield

$$r = \left(\frac{-8}{C_0 g(s-1)}\right)\frac{\partial(\beta(\tau-\tau_c)^{3/2})}{\partial x}. \tag{6}$$

It is common practice to relate the shear stress to the velocity by

$$\tau = c_f u^2, \tag{7}$$

where c_f is a dimensionless drag coefficient, typically of order 0.01. We will assume c_f to be constant.

At this point, two additional equations are required to solve the system represented by equations (2)–(7). A natural choice for the two equations would be an independent relationship between channel width and the other variables and an equation for mean grain-size as a function of x, possibly in terms of the other variables in the system, which would determine τ_c. However, there is no general relationship available for stream width. Fortunately, the need for such a relationship can also be met by postulating a relationship between the actual shear stress τ and the critical shear stress τ_c. For gravel-bed rivers with non-cohesive banks, a situation that in nature is usually associated with braiding, Parker (1978) has shown that the stress at the channel centre cannot exceed the critical value by more than a fixed, small fraction without causing bank erosion. Thus

$$\tau = (1+\varepsilon)\tau_c, \tag{8}$$

where ε is a constant. The theoretical value of ε is about 0.2; measured values are typically about 0.4 (Parker, 1978). We will refer to equation (8) loosely as the 'braided' case.

On the other hand, streams with strong cohesive and/or vegetated banks can sustain shear-stress values that are much higher than critical, especially if they have sand beds. In this case it is reasonable to assume $\tau \gg \tau_c$ such that

$$\tau - \tau_c \doteq \tau. \tag{9}$$

These conditions are likely to be met in deep, single-thread channels with well-developed flood plains. In most natural cases, such streams would be meandering. We will refer to equation (9) loosely as the 'meandering' case.

Introducing (8) or (9) into (6) gives

$$r = \left(\frac{-8A}{C_0 g(s-1)}\right)\frac{\partial(\beta\tau^{3/2})}{\partial x}, \tag{10}$$

where A is a non-dimensional constant; $A=1$ for the meandering case and $A=(\varepsilon/(1+\varepsilon))^{3/2}$ for the braided case.

Time averaging

Since we are interested in modelling the dynamics of sedimentary basins over geological time scales, the instantaneous balance equations developed so far must be time-averaged. We assume the existence of an averaging time that is long compared with individual channel-forming events but short compared with time-scales of geological interest, and denote averages over this time-scale by angle brackets $\langle\ \rangle$. The rate of deposition then becomes

$$\sigma + \frac{\partial\langle\eta\rangle}{\partial t} = \langle r\rangle, \tag{11}$$

where σ is the subsidence rate $[\Lambda\Theta^{-1}]$, taken as positive for subsidence and negative for uplift. Since all the relationships developed so far involve instantaneous variables, we must find a way of relating instantaneous to time-averaged variables. The simplest possible relationship is obtained by assuming that the flow can be characterized by a set of representative 'channel-forming' conditions that occur intermittently. This intermittency is embodied in a dimensionless time fraction I, so that

$$\langle q_s\rangle = Iq_s \text{ and } \langle q\rangle = Iq \tag{12a}$$

whereas variables that are non-zero only during a flood are unchanged by the averaging:

$$\langle u\rangle = u;\ \langle\beta\rangle = \beta;\ \langle h\rangle = h; \text{ etc.} \tag{12b}$$

This is clearly an oversimplication, but the price of added realism (for instance, treating the flow probabilistically and averaging over many realizations to yield the long-term behaviour) would be increased computational complexity, added parameters that are difficult to constrain, and the blurring of first-order effects that should be clearly understood before more complex models are developed.

An additional problem that arises with a full probabilistic treatment of flow events is that non-linear terms in the governing equations produce additional terms when averaged. For example, βq_s, which appears in equation (4), would give:

$$\langle\beta q_s\rangle = \langle\beta\rangle\langle q_s\rangle + \langle\beta' q_s'\rangle, \tag{13}$$

where primes denote deviations away from the average, i.e. $\beta' = \beta - \langle\beta\rangle$. The simplified model of intermittent but identical channel-forming events that we have adopted in (12) automatically makes the fluctuation term $\langle\beta' q_s'\rangle$ zero. More realistically, if the width is positively correlated with discharge, the fluctuation term will be positive, and its magnitude will depend both on the magnitude of width and discharge fluctuations and on the correlation coefficient between them.

Each of equations (2)–(10) has a time-averaged version determined using (11) and (12). Rather than repeating them all, here are (for example) the time-averaged versions of (2) and (4), respectively:

$$\langle q\rangle = I\beta h u; \tag{14}$$

$$\sigma + \frac{\partial\langle\eta\rangle}{\partial t} = \left(\frac{-1}{C_0}\right)\frac{\partial(\beta\langle q_s\rangle)}{\partial x}. \tag{15}$$

Combining equations (2)–(12), with time averaging we have

$$\sigma + \frac{\partial\langle\eta\rangle}{\partial t} = \frac{\partial}{\partial x}\left(v\frac{\partial\langle\eta\rangle}{\partial x}\right), \tag{16a}$$

which is the standard linear diffusion equation with the subsidence rate σ appearing as a sink term and the diffusivity v $[\Lambda^2\mathrm{T}^{-1}]$ given by

$$v = \frac{-8\langle q\rangle A\sqrt{c_f}}{C_0(s-1)} \tag{16b}$$

Note that v has two possible values depending on the value of A; for the case $A=1$, our derivation is similar to that of Begin *et al.* (1981). For a reasonable ε of 0.4 the braided-stream value of v is lower than the meandering value by a factor of about 0.15.

The drag coefficient (c_f), the sediment concentration (C_0), and the sediment specific gravity (s) can be constrained by data from modern river systems and/or preserved sediments. In any case these parameters are not expected to vary much relative to $\langle q\rangle$, the long-term average rate of water supply. It is $\langle q\rangle$ and A that primarily determine the order of magnitude of v. In other words, wet basins transport sediment more effectively than do dry basins, and deep single-thread streams transport sediment more effectively than shallow braided streams. Unfortunately, although stream type can be readily constrained using classical techniques of facies analysis, $\langle q\rangle$ is not easy to estimate from the sedimentary record. We will discuss methods of estimating $\langle q\rangle$ at the end of the paper.

In general, one would expect $\langle q\rangle$ to be an increasing function of x because of tributary input. In this paper, we will ignore this effect and treat v as a constant. Qualitatively, one important effect of including variable discharge would be to make the computed surface profiles more concave than they appear in this paper.

It is worth noting that for a stream that remains entirely within either the braided or meandering regimes as defined above, equation (16) does not depend on grain-size. This is unlike equation (6), which depends on grain-size via τ_c. As will be discussed below, the primary control on grain-size variation is the distribution of rate of deposition; the fact that equation (16) is independent of grain-size means that deposition and grain-size have been decoupled, so the distribution of deposition can be found first and the grain-size variation computed from it directly. In reality v must depend to some extent on grain-size because the channel morphology (braided versus meandering) must depend in

part on grain-size. The simplest next step would be to introduce a model for the braided-to-meandering transition, which would depend in some way on grain-size. We have not done this here mainly because it would make the computations considerably more complex without changing the results fundamentally.

Being of second order, equation (16) requires specification of two boundary conditions. The first involves the sediment flux at the upstream end of the system (Fig. 1). In previous analyses, the sediment flux has been set by coupling the depositional system of some sediment-source model, such as a diffusively eroding thrust front (Jordan & Flemings 1990), which results in a coupling between sediment flux and subsidence. We prefer to retain the sediment flux as an independent variable for two main reasons: (1) we are interested in exploring the general nature of basin response to variation in input parameters; uncoupling the flux from a specific input model such as a diffusively eroding thrust widens the range of possibilities we can study; and (2) sediment input to a basin may not be derived from directly adjoining uplifts (Dickinson 1988; Heller *et al.* 1992), in which case there seems to be no reason to couple sediment flux and subsidence. In general, the influence of each independent variable can be understood most clearly if the inputs are varied separately. It is straightforward, however, to covary any subset of the input variables in order to simulate a specific situation.

The flux is used to set the surface slope at the upstream end ($x=0$):

$$\frac{\partial\langle\eta\rangle}{\partial x} = \frac{-\langle q_s\rangle_0}{v} \text{ at } x=0, \tag{17a}$$

where $\langle q_s\rangle_0$ is the input sediment flux. The second boundary condition, applied at the downstream end of the deposit ($x=L_d$), is a bit trickier; it depends on what assumption is made about the erodibility of the basement and on whether or not the basin is overfilled ($L_d > L$). Here we assume that the basement is much less erodible than the basin fill. With this assumption we consider first the underfilled case $L_d < L$, for which the downstream boundary condition depends on the geometry of the distal end of the basin.

If the deposit is not bounded by a vertical wall, the downstream boundary condition has two independent parts: both the sediment flux and the sediment thickness must *independently* be zero (Fig. 1). The first condition says that all sediment is accounted for within the computational grid; the second, that the deposit cannot end in a cliff or fall below the basement. Actually, the flux cannot quite vanish at $x=L_d$, since there is still water flow there and we have assumed that $\tau > \tau_c$ in deriving (16). The assumption of zero flux is a convenient approximation to a small but unknown flux at the downstream end. Physically, this flux would represent sediment passed into a trunk stream flowing normal to the plane of the calculations. None of the results presented herein are changed if a nonzero flux is applied at $x=L_d$, as long as this flux is small compared with the input flux.

Thus

$$\frac{\partial\langle\eta\rangle}{\partial x} = 0 \text{ and } \langle\eta\rangle = G \text{ at } x = L_d, \tag{17b}$$

where G is the elevation of the basement [Λ]. The presence of three boundary conditions in a second-order system allows determination of one additional variable, in this case the length of the deposit L_d.

If the basin ends with a vertical wall, then the deposit thickness at the downstream end is not constrained to be zero as long as the deposit remains within the confines of the basin. In this case the third boundary condition is replaced by the requirement that the deposit length L_d be equal to the basin length L.

If the basin is just filled or overfilled ($L_d \geq L$), water and sediment continue to flow indefinitely in the same direction and the deposit does not have a well-defined length. In this case, the appropriate boundary condition is

$$\langle\eta\rangle = G \text{ as } x \to \infty. \tag{17c}$$

2.3 Modelling grain-size variation

It has long been thought that the primary mechanism of downstream fining in rivers is abrasion of coarse clasts (Krumbein 1941; Plumley 1948; Kuenen 1956). This view is partially substantiated by observations of systematic downstream change in clast composition in natural rivers, in which less durable clasts are progressively depleted (Abbott & Peterson 1978; Shaw & Kellerhals 1982). However, several workers (Shaw & Kellerhals 1982; Brierley & Hickin 1985) have noted that (1) observed rates of fining in natural rivers are often orders of magnitude higher than appears possible for abrasion alone, based on tumbling-barrel experiments; and (2) the rate of fining increases with the rate of deposition, with the highest fining rates observed on rapidly aggrading alluvial fans. The first observation can be explained to some extent by invoking abrasion processes difficult to replicate in the laboratory (Bradley 1970; Schumm & Stevens 1973), but the two observations together leave little room for doubt that selective deposition is the dominant cause of downstream fining in aggrading systems.

Unfortunately very little is known of the actual mechanics of this selective-deposition process, although work is beginning on the problem (Paola & Wilcock 1989; Parker 1991a, b; Parker, in press). Rather than attempting to incorporate an incompletely understood selective-deposition mechanism in our model, we have chosen to use a simple mass-balance approach to embody the role of selective deposition in fractionating the input sediment. In this 'perfect sorting' approach (Paola 1988, 1990), each grain-size is assumed to be deposited until it is exhausted, at which point deposition of the next size begins, and so forth, until the end of the deposit is reached. For an input size probability-density $p(D)$ [Λ^{-1}], mass conservation for each grain-size D [Λ] then implies:

$$\frac{\partial D}{\partial x} = \frac{[\sigma + \partial\langle\eta\rangle/\partial t]}{p(D)\langle q_s\rangle}. \tag{18}$$

If one is interested only in the limit of progradation L_g of the coarsest fraction of the supplied material, here taken to be gravel, then (18) is replaced by the simple mass-balance requirement that

$$f_g\langle q_s\rangle = \int_0^{L_g}\left[\sigma + \frac{\partial\langle\eta\rangle}{\partial t}\right]dx, \tag{19}$$

where f_g is the fraction of gravel in the sediment supply.

2.4 Scaling the equations

Before solving equations (16), (17), and (19), it is helpful to rewrite (16) in non-dimensional form. The basic idea of this kind of preliminary analysis of the equations, which is sometimes called 'scaling analysis', is that, although the exact value of each variable at each point cannot be known without solving the equations, it is often reasonable to assume that the *order of magnitude* of each variable will be comparable to some basic constant of the system. This constant is called the 'scale' for that variable; for instance, we expect that the scale of x will be L, the basin length. The strategy is to non-dimensionalize each variable with its scale; then all the derivatives become non-dimensional and, if the scales have been chosen correctly, of order 1. Each derivative has associated with it a group of (dimensional) constants. By rearranging an equation in this way, we have divided the information in it into two parts: the group of constants that multiplies each term carries information about the dimensions and order of magnitude of the term, whereas the derivatives determine the detailed shape of the solution in space and time. Analysis of the scaling terms allows us to anticipate features of the general behaviour of the system before a detailed solution is determined numerically, and to understand physically these detailed solutions once they are in hand.

The scale for each variable need not be known at the outset. For instance, in the present case, it is not obvious what the scale for the elevation η should be; we simply assume the existence of a reference elevation H that is of the order of η. Adopting, in addition to H and L, the characteristic scales T and σ_0 for t and σ, respectively, and by denoting non-dimensional variables with an asterisk, we have from (16)

$$(\sigma_0)\sigma_* + \left(\frac{H}{T}\right)\frac{\partial\eta_*}{\partial t_*} = \left(\frac{vH}{L^2}\right)\frac{\partial^2\eta_*}{\partial x_*^2}, \tag{20}$$

where all variables are to be taken as long-term averages. The meaning of this equation is clearer if we rearrange it using the term on the right-hand side (the rate of deposition) as a reference:

$$\left(\frac{\sigma_0 L}{Q_s}\right)\sigma_* + \left(\frac{L^2}{vT}\right)\frac{\partial\eta_*}{\partial t_*} = \frac{\partial^2\eta_*}{\partial x_*^2} \tag{21}$$

where Q_s is a characteristic transport rate $[\Lambda^2\Theta^{-1}]$ equal to vH/L. Two dimensionless numbers determine the magnitudes of the sink term and the time-dependent term relative to the sedimentation rate on the right. The first non-dimensional number, $\sigma_0 L/Q_s$, is a measure of the rate at which cross-sectional area is created in the basin (numerator) relative to the rate of sediment transport and hence basin filling (denominator). The inverse of the first nondimensional number is approximately equal to the *capture ratio* of Paola (1988): the ratio of sediment flux to the rate of creation of cross-sectional area in the basin. Roughly, if $\sigma_0 L/Q_s > 1$, the basin is underfilled; if < 1, the basin is overfilled and sediment exits the far end of the basin. In the limiting case of $\sigma_0 = 0$, no basin forms and (21) reduces to the standard diffusion equation as applied in geomorphic modelling.

The second dimensionless number on the left side of (21), L^2/vT, can be viewed as defining an intrinsic equilibrium time $T_{eq} = L^2/v$ for the basin. The presence of the time-scale in the denominator implies that if the basin is set up in some initial configuration and allowed to develop under constant conditions, then as $t\to\infty$ it will evolve toward an equilibrium (steady-state) configuration. The simplest form of equilibrium is that developed when the sediment supply is just sufficient to keep the basin filled; in this case the sedimentation rate balances subsidence at equilibrium:

$$\sigma = v\frac{\partial^2\langle\eta\rangle}{\partial x^2}. \tag{22}$$

If the basin is underfilled, then at equilibrium the sedimentation rate is constant in time but less than the subsidence rate, so that the sediment surface continues to subside. If the basin is overfilled, no steady-state configuration exists, although within the basin the sedimentation rate asymptotically approaches (22).

The time required for the basin to reach equilibrium is of the order of $T_{eq} = L^2/v$. Now let T represent the time-scale on which one of the independent forcing parameters of the basin (e.g. sediment flux or water supply) varies. If T is long relative to T_{eq}, then the subsidence term remains at least comparable to the time-derivative term $\partial\eta/\partial t$ and the basin responds to the imposed changes in what might be termed a 'quasi-equilibrium' manner.

By analogy, one might think that for rapid changes, for which $T \ll T_{eq}$, the right-hand side of equation (21) (the spatial derivative) could be neglected. However, removing the spatial derivative would reduce the order of (21), and it could no longer satisfy all of its boundary conditions. This apparent contradiction can be resolved only if a new, smaller length-scale (L') arises, such that $(L')^2/vT$ is of order 1. (Remember that the spatial derivative was set to order 1 in the non-dimensionalization.) L' is the length scale over which the effects of the fluctuations are felt in the basin; we can infer that the extent of the basin that can be affected by fluctuating conditions at one of its boundaries is proportional to the square root of the period of the fluctuations. L' becomes comparable to L when the period of the imposed fluctuations becomes comparable to T_{eq}. Note also that if L is replaced by the new reduced length scale $L' = \sqrt{vT}$ in the scaling term $\sigma_0 L/Q_s$ for subsidence, the subsidence term becomes small relative to the other

two as the time-scale diminishes. Thus, as the time-scale for imposed variations becomes short, (21) can be expected to behave increasingly like the classical diffusion equation as it is applied to geomorphic problems.

The foregoing analysis suggests that when a basin is subjected to cyclic changes in forcing parameters, the non-dimensional ratio T/T_{eq} determines which terms in the governing equation dominate the basin response. Thus one might expect that T_{eq} would be important in determining the qualitative form of basin response to imposed variations. We will refer to variations on time scales greater than and less than $T_{eq}=L^2/v$ as 'slow' and 'rapid' variations, respectively, and we give an example calculation of the relevant scales in the next section. We stress that, in thinking about T_{eq}, one must remember that it comes from a very general scaling analysis of the governing equations aimed at determining the relative orders of magnitude of the various terms. The ratio T/T_{eq}, although it is precisely defined, is not a parameter with high-precision significance; rather, it is an order-of-magnitude discriminator between two broad regimes of basin response. In that sense, it is like the Reynolds and Froude numbers in fluid mechanics.

2.5 Estimation of scales

As mentioned above, most of the elements of the diffusivity are fairly well constrained. Adopting as reasonable values $c_f=0.01$, $C_0=0.7$, $s=2.7$, and $\varepsilon=0.4$, we have for the braided case $v=0.10\langle q\rangle$ and for the meandering case $v=0.67\langle q\rangle$. The average water discharge per unit width of basin $\langle q\rangle$ is rL_c, where r if the rainfall rate and L_c the length of the catchment area (note that we are ignoring downstream changes in $\langle q\rangle$ due to rainfall along the basin itself). For a catchment length of 10^5 m and a rainfall rate of 1 m yr^{-1} we have for the braided case, a diffusivity of 1×10^4 m^2 yr^{-1} and for the meandering case 7×10^4 m^2 yr^{-1}. If the basin length is comparable to the catchment length (10^5 m) then the equilibrium time of the basin L^2/v is of the order of 10^6 yr in the braided case and 10^5 yr in the meandering case. In general, if the catchment length and the basin length are of similar order of magnitude then the equilibrium times are of the order $10L/r$ for the braided case and $1.5L/r$ in the meandering case.

2.6 Method of solution

There are a variety of numerical methods available for solving equation (16); we use a fully implicit method (Press *et al.* 1986, p. 637) to allow for long time steps. The major problem in finding the solution is determining the length of the deposit for each time step. This arises because the position of the boundary must be determined as part of the solution to (16) for each time step. Usually the boundary can be expected to lie somewhere between the nodes of the computational grid. We have found, however, that positioning the boundary on the nearest node of a fixed grid produces acceptably small errors in mass conservation (typically a few percent over 100 times steps), provided the grid is reasonably fine. For the calculations discussed below, we used a grid with 100 spatial steps.

In this paper we have solved equation (19) for L_g to determine the position of a single grain-size front (the limit of transport of material coarser than some given size) through time. It is important to note that at each time step the gravel flux in (19) must be corrected to account for the grain-size content of any sediment eroded within the basin as well as the material supplied from outside.

2.7 Limitations of the model

Most of the important limitations of the model developed in this paper are clear from the assumptions we have made in deriving it. We make no attempt to predict the fine details of facies distributions, nor do we attempt to predict stochastic properties of stratigraphic response. The two-dimensionality of our model is a limitation in two senses. The obvious one is that we cannot treat basins with three-dimensional geometry (either three-dimensional subsidence or multiple sources of sediment); the model also cannot describe the whole of a system with three-dimensional drainage, although many of the results do apply to the two-dimensional feeder part of such a system. A more subtle limitation imposed by two-dimensionality is that both deposition and erosion are assumed to occur over the entire width of the depositional system. This is probably a more reasonable assumption for deposition than for erosion, especially at short time scales, where erosion is usually associated with local valley incision. Some of these effects can be incorporated in two-dimensional models, but clearly three-dimensional models will be required ultimately.

Another general limitation of the model is that, in the interests of understanding clearly the first-order dynamics, we have left out a number of the details of fluvial processes. In general, the effects of our simplifications are likely to be most important for short time scales. Ribberink & Van Der Sande (1985) have studied the behaviour of rivers over a range of time and space scales, focusing on the effects of non-linear terms in the momentum equation for subcritical flows. They find that diffusion models become valid for length and time scales above certain limiting values: the limiting length scale is about $7h_0/S_0$, where h_0 and S_0 are a characteristic water depth and bed slope, respectively; the limiting time scale is about $2h_0^2/(S_0q_{s0})$, where q_{s0} is a characteristic sediment transport rate. For time and space scales below these limiting values, the bed shows various types of wave-like behaviour.

In general, the limiting scales above which a river system behaves diffusively are probably below the resolution of first-order models for steep, shallow stream systems but are significant for deep, low-gradient streams. For example, for a stream 1 m deep flowing on a slope of 10^{-3}, the critical length for diffusion is about 7 km. However, a river 10 m deep flowing on a slope of 10^{-4} would have a critical length of 700 km; in that case, non-diffusional (wavelike)

Table 1. Values used for model runs

We used the following values in all runs (Figs 2, 4, 5, 6 and 7)
Mean capture ratio: 1.0
Mean diffusivity: 1×10^{-2} km^2 yr^{-1}
Mean supply gravel fraction: 0.3
Basin length L: 100 km
Equilibrium time T_{eq}: 10^6 yr
Form of imposed variation: $v(t) = \bar{v}*(1 + 0.7*\sin(2\pi t/T))$
(where t is time; T is period; v is any of the four basic independent variables: sediment flux, subsidence rate, gravel fraction, or diffusivity; and $\bar{v}$ is the mean value of the variable).

For all the runs, the numerical solution to equation (16) was carried out as follows:
Spatial grid interval: 1 km
Time interval: $T/100$
Solution method: fully implicit

For runs with linearly increasing subsidence (Figs 2, 4, and 5) we used
Mean subsidence rate: 5×10^{-7} km yr^{-1}
Mean sediment flux: 5×10^{-3} km^2 yr^{-1}

For runs with spatially constant and decreasing subsidence (Fig. 7) we used
Mean subsidence rate: 1×10^{-6} km yr^{-1}
Mean sediment flux: 1×10^{-4} km^2 yr^{-1}

For slow variation (Fig. 2) we used:
Period of variation T (all 4 variables): 1×10^7 yr
Interval between time lines: 1×10^6 yr

For rapid variation (Fig. 4) we used:
Period of variation T (all 4 variables): 1×10^5 yr
Interval between time lines: 1×10^4 yr

For equilibrium variation (Fig. 5) we used:
Period of variation T (all 4 variables): 1×10^6 yr
Interval between time lines: 1×10^5 yr

behaviour could not be ignored even in large-scale basin models.

3 MODEL RESULTS FOR SLOW VARIATIONS

3.1 General aspects of the model runs

In the model runs, the basin length and average diffusivity are those given for the braided case (10^5 m and 10^4 m^2 yr^{-1}, respectively). All values used in the runs are given in Table 1. We consider variation in each of the four basic governing parameters: sediment flux, subsidence rate, gravel fraction in the sediment supply, and diffusivity (controlled primarily by the rate of water supply). The amplitude of the variation is 70% of the mean value in each case. The mean value of the capture ratio is 1, so on average the basin is just kept filled with sediment. We use equation (19) to determine the location of a single grain-size transition, which we will take to be from gravel to sand.

In all the runs discussed in this paper, the basin is allowed to fill with sediment under constant conditions for a period equal to four times the equilibrium time before the variation is begun. At the end of this period, the variation begins. The variables change as $\sin(2\pi t/T)$, where t is time and T is the period of the fluctuations. Once the variation begins, time lines are drawn every $0.1T$.

In all the runs presented in the next three sections, the subsidence profile is linear with the hinge point at the distal end of the basin. This subsidence model is unrealistically simple, but it streamlines the computations and is adequate to reveal the basic effects of varying the subsidence rate as well as the other three parameters listed above. Since the subsidence model is not the main focus of this paper, we also ignore coupling between the sediment load and subsidence; that is, we have not accounted for the common observation that sediment deposition loads the lithosphere and thus increases the subsidence rate. More detailed examination of the effects of sediment loading in flexural basins can be found in recent works by Moretti & Turcotte (1985), Kusznir & Karner (1985), and Flemings & Jordan (1989).

We begin by presenting model results for slow variations; that is, those for which conditions vary on a time-scale T such that $T/T_{eq} \gg 1$. The variation occurs on a time-scale of 10^7 years, 10 times the equilibrium time, and time lines are drawn every 10^6 yr.

3.2 Variation in sediment flux

Figure 2a shows the results of a model run as described above in which the sediment flux varies sinusoidally and all other variables are held constant. Vertical sedimentation rates increase as sediment flux increases, as shown by an increase in spacing between isochrons on the diagram. Clastic progradation occurs (the position of the gravel–sand transition migrates towards the basin centre as the sediment flux increases. Clastic progradation over time is, of course, accompanied by an overall grain-size increase in any vertical section measured in the basin. Thus, this 'flux-driven' style of progradation shows a positive correlation between sediment accumulation rate and grain-size in vertical sections across the basin.

This scenario represents the traditional 'syntectonic' interpretation of coarsening-upwards sections and gravel progradation in alluvial basins (Rust & Koster 1984). An increase in tectonic uplift in the source area would increase source-area relief and thus increase sediment flux to the basin. However, insofar as sediment flux is also affected by climate and source-rock type, one could produce the same response pattern through a non-tectonic mechanism.

3.3 Variation in subsidence rate

A second model run (Fig. 2b) shows what happens if basin subsidence rate varies sinusoidally while the other variables remain constant. As subsidence begins to increase, more accommodation space is generated, trapping the supplied sediment in the most proximal part of the basin while the most distal sediments are eroded. The coarsest sediment, being the first to deposit, is localized in the extreme upstream end of the basin. Locally, vertical sedimentation rates in the proximal part of the basin increase as the gravel–sand transition migrates towards the proximal end of the basin, in accordance with equation (19). The mean subsidence rate then decreases, space available for deposition decreases, and the gravel-sand transition progrades out across the basin. As in the previous case, this progradation is associated with an increase in grain-size in any vertical section. But for this 'subsidence-driven' case, an increase in grain-size upsection is associated with a reduction in vertical accumulation rate – exactly the opposite of the flux-driven case described above.

The subsidence-driven case is one in which gravel progradation is linked to a reduction in local sediment accumulation rate. If the subsidence rate is directly related to tectonic activity, then subsidence-driven gravel progradation represents periods of *diminishing* tectonic activity; this case might be termed 'antitectonic' progradation. Note, however, that gravel progradation could be subsidence-driven and yet syntectonic if the tectonism involved reduction in subsidence rate. Such a case was posited by Burbank & Raynolds (1988), who argued that blind thrusts and folds caused local reductions in subsidence rate during Himalayan thrusting.

3.4 Variation in gravel fraction

The third case we consider is that in which gravel progradation is caused by an increase in the fraction of gravel in the sediment supply. Such an increase could occur because of a change in source-rock lithology, or a change in climate. In this case (Fig. 2c), sediment flux and subsidence rate remain constant and thus the grain-size changes upsection while the vertical sedimentation rate remains constant. In this 'distribution-driven' model, there is no correlation between vertical change in grain-size and accumulation rate.

3.5 Variation in water supply

As discussed above, the amount of water available to the basin is reflected directly in the diffusivity. The results of varying the diffusivity sinusoidally can be seen in Fig. 2d. Although the amplitude of variation is just as large as for the variables discussed above, the imposed change in diffusivity has almost no effect on the pattern of fill in the basin. We will discuss the reason for this in detail below, but the basic idea is that changes in diffusivity affect only the sediment surface. On long time-scales, the subsidence is much more important than the surface elevation in the overall mass balance of sediment, so variation in diffusivity has relatively little effect.

3.6 Summary

Clearly, on time-scales that are long relative to T_{eq}, changes in sediment flux, subsidence rate and sorting cause the position of the gravel-sand front to shift smoothly across the basin. The end-member models discussed above are distinguished by the relative timing of changes in grain-size and vertical accumulation rate (Fig. 3). In the flux-driven case, sedimentation rate and grain-size change in phase with one another (Fig. 3a). For the subsidence-driven case, sedimentation rate and grain-size are exactly out-of-phase (Fig. 3b). In the distribution-driven case, there is no phase relation between grain-size and sedimentation rate (Fig. 3c). In contrast to these three cases, changes in water supply have no effect when applied over long time-scales.

4 MODEL RESULTS FOR RAPID VARIATIONS

The runs in this section were done to examine the basin response to rapid variations in the forcing parameters; that is, variations with a period T such that $T/T_{eq} \ll 1$. The runs discussed below were made under the same conditions as those above except that the period of variation T is 10^5 yr, a factor of 100 less than those of the previous section and a factor of 10 less than the equilibrium time. Time lines in this section are drawn every 10^4 yr.

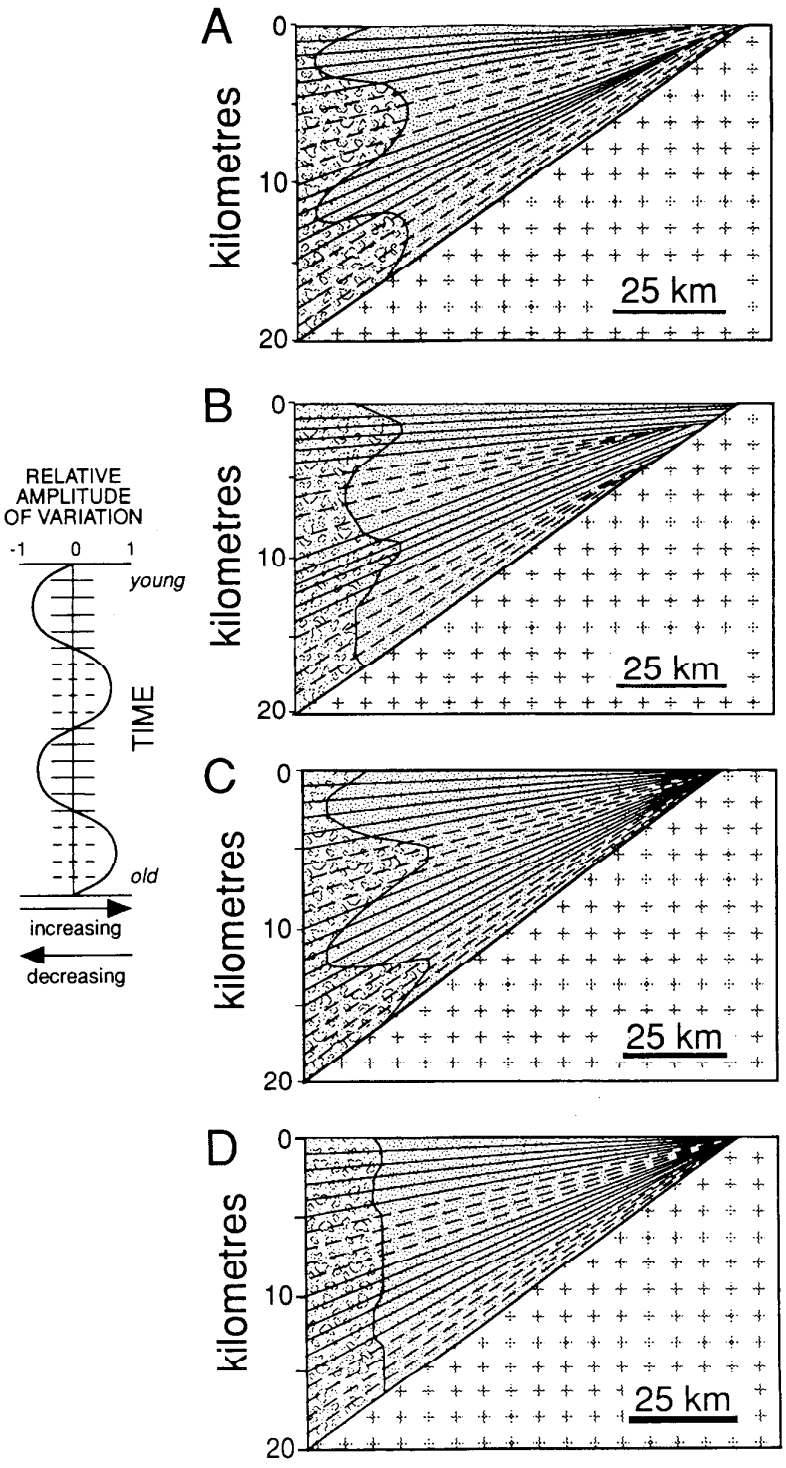

Fig. 2 Cross-section of a hypothetical basin showing the results of slow variation ($T \gg T_{eq}$) in (a) sediment flux, (b) subsidence, (c) gravel fraction, and (d) diffusivity. Gravel is shown in dark grey, sand in light stipple. Direction of transport is from left to right. The thin dashed and solid lines are isochrons drawn every 10^6 yr; the heavy lines show the basement. The form of the variation is shown at left and is the same for all parameters; the intervals represented by dashed time lines represent maxima in the forcing parameter. The conditions of the run are given in the text and in Table 1.

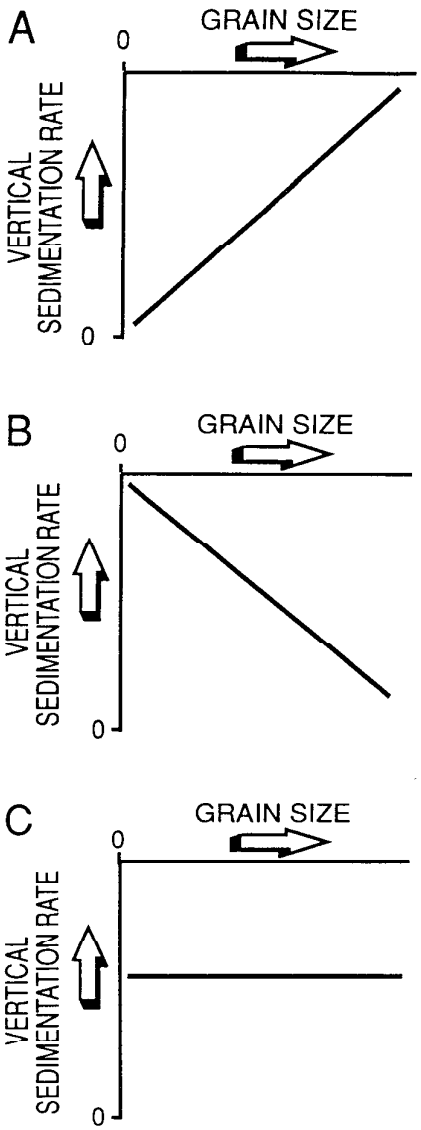

Fig. 3 Sketch graphs showing the relation between grain-size and local sedimentation rate for (a) flux-driven, (b) subsidence-driven, and (c) distribution-driven coarsening.

4.1 Variation in sediment flux

The results of rapid variation in sediment flux are shown in Fig. 4a; they are quite different from the slow case. During times of reduced sediment flux, the upstream part of the system is eroded as slopes are reduced to accommodate the decreasing flux. This results in the generation of proximal unconformities and the dispersal of gravel far out into the basin. Thus, in contradistinction to the slow case (Fig. 2a), rapid variation in sediment flux results in gravel progradation during times of *reduced* sediment flux. Furthermore, the form of the gravel bodies is quite different: even though the imposed variation is smooth and sinusoidal, the progradation takes place abruptly, leading to a distinctive sheet-like geometry. The retrogradation is even more abrupt, giving the whole cycle an asymmetric, coarsening-up form. In addition, gravel progradation is associated with pronounced proximal unconformities that become less well developed going out into the basin.

4.2 Variation in subsidence rate

The results of rapid variation in subsidence rate are shown in Fig. 4b. The general form of the basin response is similar to that for slow variation in that the gravel front progrades during times of reduced sedimentation rate. However, for the same magnitude of subsidence variation, the response of the sedimentation rate and position of the gravel front is much weaker for rapid than for slow variation, and the time of maximum progradation is phase-shifted somewhat so that it takes place when the subsidence rate is increasing rather than when it is at a minimum.

4.3 Variation in gravel fraction

Rapid variation in gravel fraction of the input sediment, illustrated in Fig. 4c, produces an effect almost identical to slow variation in gravel fraction: the gravel front progrades smoothly and continuously, and there are no accompanying changes in sedimentation rate.

4.4 Variation in water supply

The results of varying the diffusivity (and hence the rate of water supply) rapidly are shown in Fig. 4d. In striking contrast to the results for slow variation, rapid changes in diffusivity produce strong effects similar to those of rapid variation in sediment flux: times of increased diffusivity, like times of reduced sediment flux, produce strong proximal unconformitiess and thin, extensive gravel tongues; the maximum extent of gravel progradation occurs just before the maximum water flux, when the latter is still increasing. The progradation is abrupt even though the imposed variation is smooth and sinusoidal.

5 MODEL RESULTS FOR EQUILIBRIUM VARIATIONS

Having examined basin response to sinusoidal variation in forcing parameters for the two end-member cases of slow and rapid variation, it is of interest to consider what happens when the period T of the imposed change is equal to the characteristic equilibrium time T_{eq} of the basin. Model results for this case are shown in Fig. 5. These runs were made under the same conditions as those above except that the period of variation T is 10^6 yr, equal to the equilibrium time. Time lines in this section are drawn every 10^5 yr.

In general, as one would expect, the results for equilibrium variation are intermediate between those for slow and rapid variation, although they seem in general to be closer to those for slow variation. The form of the

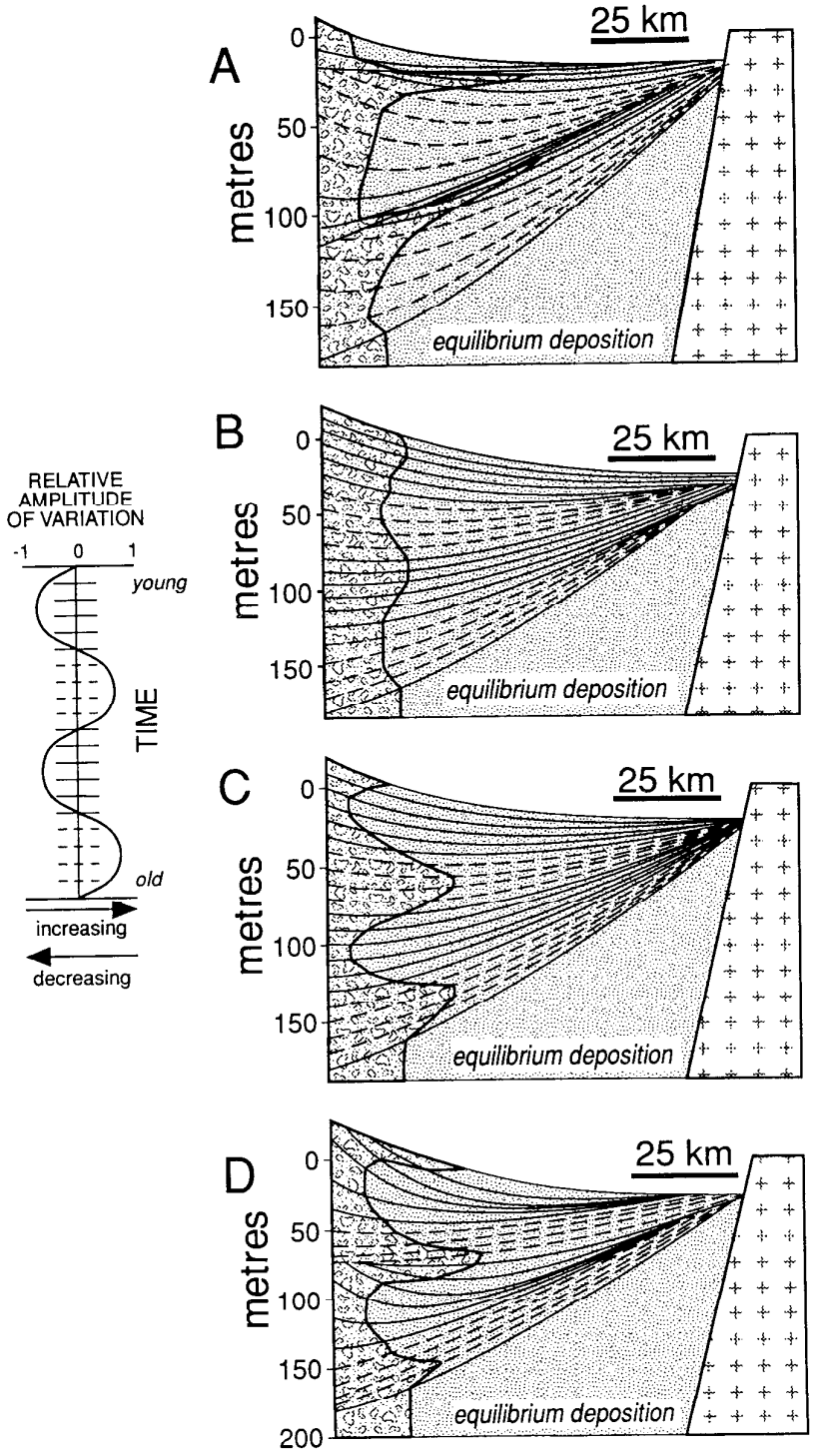

Fig. 4 Cross-section of a hypothetical basin showing the results of rapid variation ($T \ll T_{eq}$) in (a) sediment flux, (b) subsidence, (c) gravel fraction, and (d) diffusivity. Symbols are as in Fig. 2 except that time lines are drawn every 10^4 yr. The conditions of the run are given in the text and in Table 1.

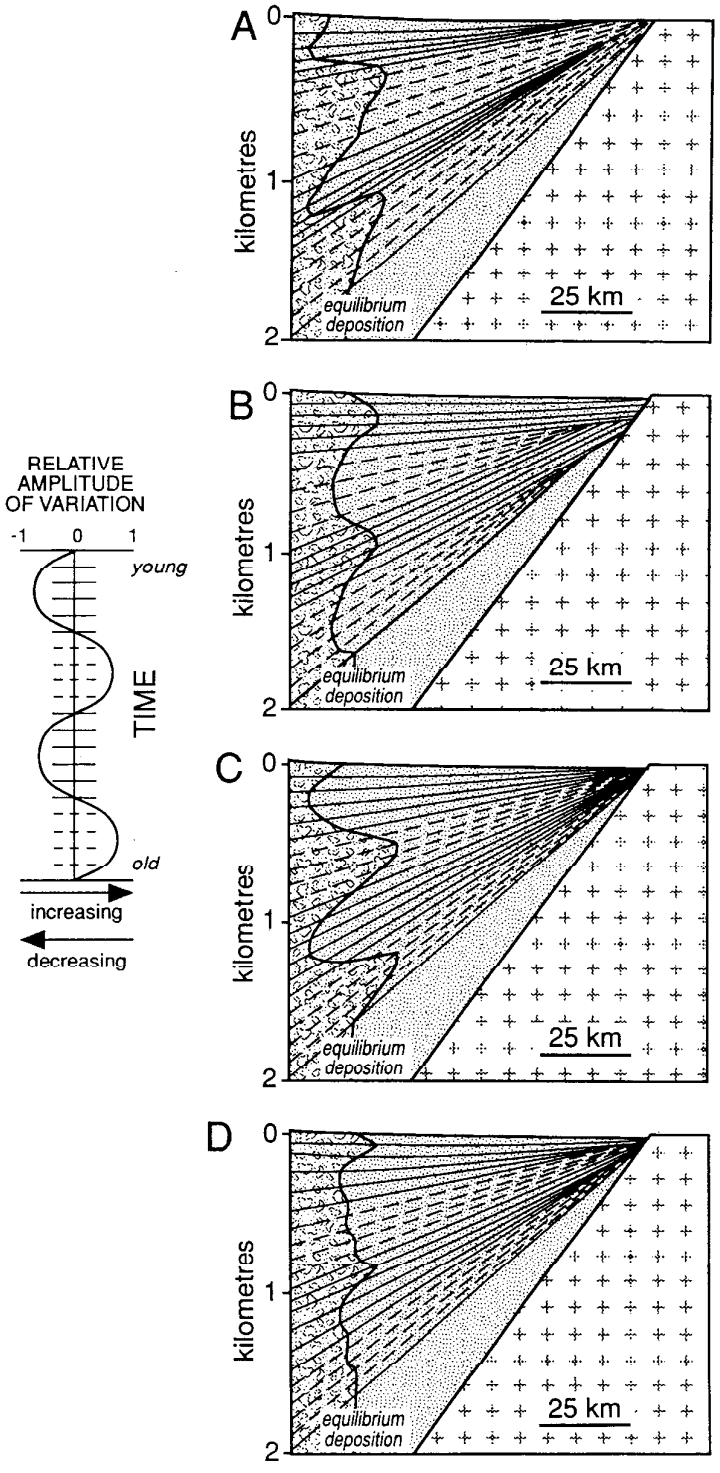

Fig. 5 Cross-section of a hypothetical basin showing the results of equilibrium variation ($T = T_{eq}$) in (a) sediment flux, (b) subsidence, (c) gravel fraction, and (d) diffusivity. Symbols are as in Fig. 2 except that time lines are drawn every 10^5 yr. The conditions of the run are given in the text and in Table 1.

response for sediment flux is distinctly more asymmetric than for the slow case, and the time of maximum progradation is shifted towards the minimum in the sediment flux. The response for subsidence is similar to the slow case, but slightly weaker. The response for gravel fraction is unchanged, and that for diffusivity shows very weak progradation during times of increasing diffusivity (recall that slow variation in diffusivity produces no effect).

Finally, it is of interest to establish how far one must be from T_{eq} to have a 'fully developed' slow or rapid response; this is especially important in estimating the influence of uncertainty in estimates of T_{eq} on interpretation of observed responses in the geologic record. We illustrate the transition from slow to rapid response as the period passes through T_{eq} using sediment flux, since the flux shows strong but distinctly different responses for slow and rapid variation. Figure 6 shows the form of gravel-front variation produced by one sinusoidal cycle of change in flux (what is shown is gravel front position traced from model-generated basin cross-sections, normalized to constant total sediment thickness), for a series of periods from slow to rapid. The characteristic form of the response to slow variation seems to be well developed by the time the period is a factor of 2 greater than T_{eq}, whereas the form of response to rapid change is not well established until the period is at least a factor of 4 below T_{eq}. The depth of proximal erosion and the distance of gravel progradation continue to increase as the period decreases, although for most basins, our model would not be expected to be accurate for periods far below T_{eq} for the reasons discussed above.

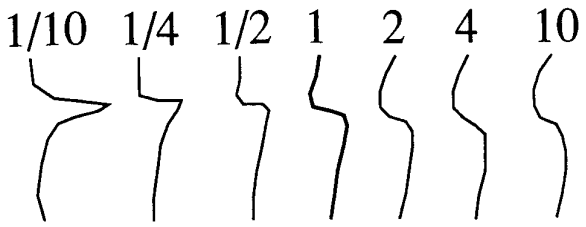

Fig. 6 The form of the response of the gravel front to changes in sediment flux as a function of T/T_{eq} (given by the fraction over each curve). The curves were traced directly from model-generated basin cross-sections (as in Figs 2, 3 and 5) for one complete cycle of variation and have been normalized to the same total sediment thickness. Input conditions were as for Figs 2, 3 and 5 except for the change in the period of variation.

6 THE EFFECT OF BASIN SHAPE

All of the results discussed so far have been obtained for basins in which the subsidence rate decreases linearly away from the sediment source; it is of interest to know whether these results would be qualitatively different for basins with different subsidence patterns. Although we have not explored all possible spatial patterns, we have replicated the runs described above for two other simple subsidence geometries: constant, and linearly increasing across the basin. For the sake of brevity, we will not reproduce all these results here. While all the variables show some change in response as the basin shape changes, only the response to subsidence variation depends qualitatively on the shape. Results for variation in subsidence rate for the two additional basin shapes are shown in Fig. 7. For spatially constant subsidence (Fig. 7a), changes in subsidence rate produce no response at any time-scale. For spatially increasing subsidence (Fig. 7b), there is a strong response to slow variation, with maximum progradation occurring during times of mimimum sedimentation rate in the proximal part of the basin, as in the slow variation discussed earlier. However, careful examination of Fig. 7b shows that the minimum proximal accumulation rate for this case occurs when the subsidence rate is a *maximum*, the exact opposite of the case with spatially decreasing subsidence. Thus, for spatially increasing subsidence, subsidence-driven gravel progradation may be 'syntectonic', if tectonic activity is correlated with subsidence rate.

The origin of this change in relation between gravel progradation and subsidence is quite subtle, and is in part an artifact of the way the model is set up. The basic issue is that because there is no fixed elevation which the sediment surface is tied, there can be no direct coupling between sedimentation rate and subsidence rate. This would not be the case if the sediment surface were matched to sea-level or some other reference elevation. However, in the absence of a base level, the only coupling between subsidence and sedimentation is through tilting of the sediment surface, which induces slope changes in the river system. In the case of spatially constant subsidence, there is no tilting, so there is no mechanism for transmitting the changes in subsidence rate to the river system, and the sediment surface simply rides up and down passively as the subsidence rate varies. In reality, increases in subsidence rate in such a system would probably be coupled to increases in erosion of the basin margins. Thus our scenario of variation in subsidence with constant sediment flux, although useful in clarifying the basic mechanics, is not very realistic for this case. This would be easy to remedy by coupling the sediment flux to the relief at the basin margin.

For the case of spatially increasing subsidence, temporal increases in subsidence rate increase the rate of tilting of the sediment surface, so they do cause increases in sedimentation rate. However, most of the increase occurs in the distal part of the basin, where the subsidence rate is highest. Since the sediment flux remains constant, this results in a net transfer of sediment from the proximal part of the basin to the distal part, reducing the sedimentation rate in the proximal part and causing gravel progradataion during times of high subsidence rate.

At the risk of overcomplicating things, we note that the foregoing discussion applies only as long as the basin does not become overfilled. If overfilling does occur, the picture is changed because the surface elevation beyond the basin then acts to provide a kind of base level for the river system, and the sediment surface can no longer ride passively up and down on the basin floor. It is beyond the scope of this paper to investigate this issue further. The important point

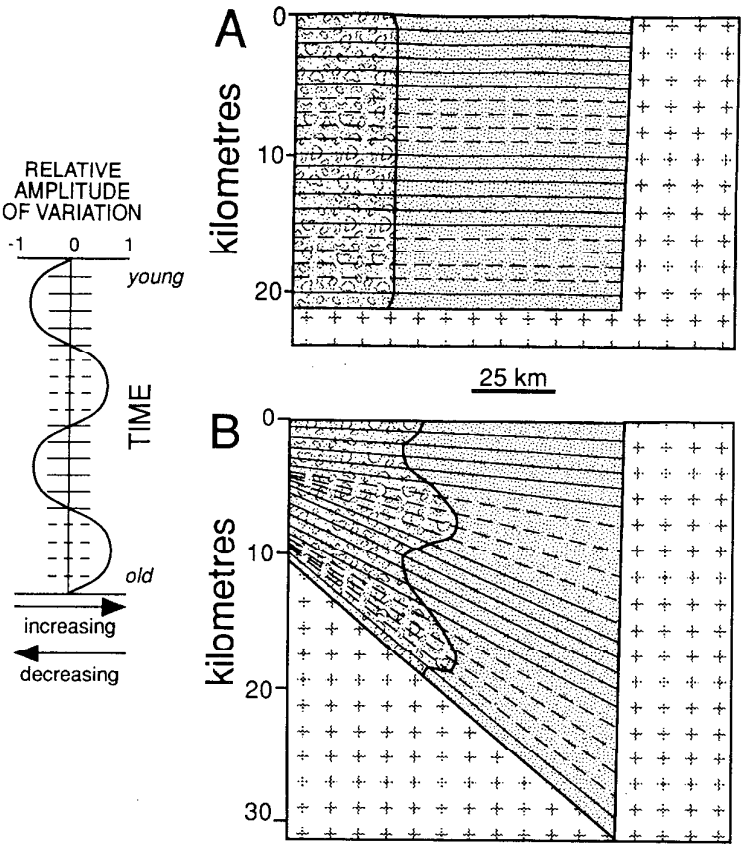

Fig. 7 Cross-section showing the results of slow variation ($T \gg T_{eq}$) in subsidence rate for basins of two different cross-sectional shapes. In (a) the subsidence rate σ is spatially constant $\sigma(x, t) = \sigma_0(t)$, and in (b) the spatial pattern is given by $\sigma(x, t) = \sigma_0(t)\,(0.5 + x/L)$, where $\sigma_0(t)$ is a reference subsidence rate and the other symbols are as defined in the text.

here is that, in subsidence-controlled migration, the one abiding constant is that progradation is always linked to decreases in the local sedimentation rate. The complications occur in the relation between subsidence rate and sedimentation rate, which is qualitatively dependent on the system geometry. In particular, some sort of fixed reference level, in the form of an elevation boundary condition on the sediment surface, is required to provide direct coupling between subsidence and sedimentation.

7 DISCUSSION

7.1 Summary and discussion of model results

For each variable except gravel fraction, the form of basin response is different for rapid variation than for slow variation. This distinction makes clear the fundamental role played by the equilibrium time in governing basin response to imposed variations, for it is the equilibrium time that determines what 'slow' and 'rapid' mean in real time. The model results are summarized below.

Slow variation in sediment flux produces smooth progradation and retrogradation of the gravel front (Fig. 2a). Progradation is accompanied by increasing local sedimentation rate so that gravel transport distance and sedimentation rate vary in phase; we term this 'flux-driven' coarsening. In contrast, rapid flux variation (Fig. 4a) produces abrupt progradation of the gravel front that forms a thin, extensive gravel sheet bounded below by strong proximal unconformities that diminish into the basin. Although the gravel progrades abruptly, retrogradation is even faster, so that overall a coarsening-upward vertical signature results.

Slow variation in subsidence rate also produces smooth progradation and retrogradation of the gravel front (Fig. 2b). Progradation is accompanied by reduction in localf sedimentation rate so that gravel transport distance and sedimentation rate are 180° out of phase; we term this 'subsidence-driven' coarsening. As the period of variation in subsidence becomes shorter than the equilibrium time, the changes in sedimentation rate induced by subsidence variation become weaker and also begin to lag behind the changes in subsidence. The position of the gravel front continues to be inversely related to the sedimentation rate, so its response to variation in subsidence is similarly weakened.

Slow and rapid variation in supplied gravel fraction produce similar effects (Figs 2c, 4c): smooth progradation (during times of high gravel supply) and retrogradation, with no accompanying changes in sedimentation rate.

Slow variation in water supply (diffusivity) produces no effect (Fig. 2d), but rapid variation produces abrupt progradational cycles (Fig. 4d), with extensive sheet-like gravel units being generated during times of increasing-to-

high water supply. The overall pattern is highly asymmetric, broadly similar to that for rapid variation in sediment flux.

It seems clear that the way basins respond to changes in their governing parameters can differ dramatically depending on the time-scale on which the changes occur. Note that the cause of the change in response from slow to rapid is the time-scale of the variation, not the sediment thickness deposited. The overall deposit thickness changes in Figs 2, 4 and 5 because we have kept the subsidence rate constant in all the calculations while changing the time-scale. An explanation for this dependence of the form of the response on time-scale can be found in the discussion of scaling effects in section 2.4. There we showed that in the long-term balance the most important terms are subsidence and sedimentation rate; changes in surface topography, although significant, remain smaller than the subsidence rate, and go to zero in the case of true equilibrium governed by (22). On the other hand, on short time-scales, the subsidence (sink) term becomes progressively less important and (16) behaves like the conventional diffusion equation involving only the surface topography. This can be summarized metaphorically by saying that slow changes are felt in the body of the basin while rapid changes are felt in its skin. Thus rapid changes in subsidence rate produce weak effects because the subsidence-rate is not that important in the short-term balance. A more intuitive way of seeing this is to note that, for changes in the subsidence rate to conrol sedimentation pattern, sediment must be redistributed across the whole basin, which becomes increasingly difficult on time scales less than the equilibrium time.

Using similar logic, slow changes in water supply (diffusivity) have no effect because they affect only the sediment surface. On long time-scales, the mass balance in the basin is dominated by sedimentation rate and subsidence, and is nearly independent of the surface topography. On the other hand, at short time-scales, surface effects predominate. Since changes in water supply have a strong effect on surface configuration, they affect the short-term pattern of sedimentation strongly. Finally, changes in sediment flux are effective on both time-scales because the sediment flux affects both the overall mass balance of the basin and the surface topography. The latter effect results from the boundary condition (17a). The reversal in form of the response to varying flux as the time-scale changes results from competition between the effect of the flux on the mass balance and on the sediment surface. Over long time-scales the mass-balance effect is more important, while on short time-scales, the surface effect predominates. Note also that, since the effect of the flux on the sediment surface originates at the basin margin and propagates basinward, the argument made in section 2.4 about reduced length scales comes into play: The length scale L' over which the variation in sediment flux can be expected to propagate goes as $\sqrt{T}$ so the effects of variation on a time scale of $0.1\,T_{eq}$ should be concentrated in approximately the upstream-most 30% of the basin. That this is indeed the case for the sedimentation rate can be seen from inspection of Fig. 4a. The gravel front propagates much farther into the interior than this, however, because of the strong increase in total gravel flux as the gravel-rich upstream deposits are eroded. In a sense, the behaviour of the gravel front amplifies the variations in sedimentation rate.

7.2 The behaviour of 'marker' clasts in the context of the model

One of the principal tools used in inferring source-area tectonic history from basin sediments, especially gravels, is the appearance in the deposit of distinct clast types ('marker' clasts) that can be unambiguously associated with a particular source-rock type (Burbank *et al.* 1988; Jordan, Flemings & Beer 1988). It is important to note that in diffusive models such as the one developed in this paper, any change in the clast composition of the source area appears *immediately* across the entire gravel deposit. In other words, if the composition of the supplied gravel clasts changed from time step t_i to time step t_{i+1}, the entire gravel unit deposited during time step t_{i+1} would reflect the new composition. This is because the diffusion model does not account for the transport dynamics of individual clasts. In the present context, the critical point is that the migration of gravel fronts as shown in Figs 2–7 has nothing to do with the speed at which individual clasts are brought to the leading edge of the front; this process is instantaneous as far as the model is concerned. Of course, in reality, marker clasts do take a finite time to propagate across the gravel depositional area. The processes that govern the appearance of marker clasts in the deposit are (1) sediment dynamics at time-scales below the resolution of the diffusive approximation, and (2) the time required for streams in the source area to erode strata contributing the marker clasts and supply them to the edge of the basin.

7.3 Applications

At this point it is not clear how one could provide a true, rigorous test of the results of even simple models such as the one we have presented here. The most immediate application of the results is as an indication of the form of response produced by variations in each governing parameter acting in isolation, and of the critical observations needed to distinguishing among them. We apply the model results to available field data in the companion paper following this one (Part 2); here we offer some general comments on applying the model results:

The four basic variables that we have studied vary dramatically in the responses they produce at different time-scales. This characteristic might be useful in designing future field studies. For instance, if basins cannot respond to changes in subsidence rate on a time scale much below the equilibrium time, then, in effect, basin sedimentation acts as a low-pass filter on subsidence changes. On the other hand, the large-scale sedimentation pattern is sensitive to changes in water supply only on time-scales shorter than the equilibrium time. Basins thus act as high-

pass filters for variations in water supply. To apply this line of reasoning to real basins, it is necessary to estimate the equilibrium time T_{eq} and for that one must estimate both basin length and diffusivity, at least to within an order of magnitude. We discuss estimation of diffusivity below. It seems reasonable, however, that at least within a single climatic zone, basin length rather than diffusivity is likely to be the main variable that determines the equilibrium time. One could then hope to sharpen both palaeoclimatic and tectonic studies by choosing basins whose sizes 'tune' them correctly to a given problem.

The results of our modelling make clear the basic role played by the long-term average water discharge in governing basin behaviour, via the diffusivity. The diffusivity is not only an important variable in its own right, but its characteristic value helps determine the equilibrium time, which is critical in determining how any other sort of variation will affect basin sedimentation. One of the great challenges of applying models such as this one to the interpretation of sedimentary rocks is to find ways of constraining the water supply. We suggest two basic avenues of approach: (1) palaeoclimatic estimation of rainfall rates (from studies of paleosols, and/or fossil assemblages) coupled with tectonic constraints on the size of the ancient drainage area; and (2) palaeohydraulic reconstruction of flow rates in ancient river systems. The first method gets directly at the critical parameter (the long-term average water supply rate), but is apt to be imprecise, especially given that drainage divides are generally located in uplifted areas and are thus likely to be eroded away. As for method (2), while fairly precise palaeohydraulic reconstructions of specific palaeoflow events are possible, it is not clear how these could be suitably integrated to give an estimate of long-term water supply. Although neither approach is ideal, we think both are worth pursuing and that together they offer an appealing way of quantitatively integrating detailed sedimentological studies with regional basin analysis.

While work continues on finding new ways of constraining the independent parameters of models such as ours, we hope that the distinctive response patterns we have found will be helpful to those interested in distinguishing among the various factors that determine the pattern of sedimentation in basins. Beyond these specific response patterns, the most important general result of our work is that the time-scale on which variations in forcing parameters occur is a fundamental variable in itself. Before one can begin to address, for example, questions of tectonic or climatic controls on sedimentation, one must first consider both the time-scale on which the change occurs and the characteristic equilibrium time of the basin in question.

ACKNOWLEDGMENTS

It is a pleasure to thank Gary Parker and Karen Kleinspehn for many helpful and enjoyable discussions. We are also very grateful to Peter Flemings, John Grotzinger, John Southard, and Julian Thorne for thoughtful and constructive reviews of this paper. Financial support has been provided by National Science Foundation grants EAR 87-07041 and EAR 89-04613.

REFERENCES

ABBOTT, P. L. & PETERSON, G. L. (1978) Effects of abrasion durability on conglomerate clast populations: examples from Cretaceous and Eocene conglomerates of the San Diego area, California. *J. sedim. Petrol.* **48**, 31–42.

ADACHI, S. & NAKATOH, T. (1969) Changes to top-set-bed in a silted reservoir. *Int. Ass. Hydro. Res. 13th Congr.* pp. 269–271.

BEGIN, Z. B. (1987) ERFUS 6—a FORTRAN program for calculating the response of alluvial channels to baselevel lowering. *Comp. Geosci.* **13**, 389–398.

BEGIN, Z. B., MEYER, D. F. & SCHUMM, S. S. (1981) Development of longitudinal profiles of alluvial channels in response to base-level lowering. *Earth Surf. Proc. Landforms* **6**, 49–68.

BLAIR, T. C. & BILODEAU, W. L. (1988) Development of tectonic cyclothems in rift, pull-apart, and foreland basins: sedimentary response to episodic tectonism. *Geology* **16**, 517–520.

BRADLEY, W. C. (1970) Effect of weathering on abrasion of granitic gravel, Colorado River (Texas). *Bull. geol. Soc. Am.* **81**, 61–80.

BRIERLEY, G. J. & HICKIN, E. J. (1985) The downstream gradation of particle sizes in the Squamish River, British Columbia. *Earth Surf. Proc. Landforms* **10**, 597–606.

BROWNLIE, W. R. (1981) *Prediction of Flow Depth and Sediment Discharge in Open Channels.* California Institute of Technology, W. M. Keck Laboratory, Report No. KH-R-43A, 232 pp.

BURBANK, D. W., BECK, R. A., RAYNOLDS, R. G. H., HOBBS, R. & TAHIRKHELI, R. A. K. (1988) Thrusting and gravel progradation in foreland basins: A test of post-thrusting gravel dispersal. *Geology* **16**, 1143–1146.

BURBANK, D. W. & RAYNOLDS, R. G. H. (1988) Stratigraphic keys to the timing of thrusting in terrestrial foreland basins: Applications in the northwestern Himalaya. In: *New Perspectives in Basin Analysis* (Ed. by K. L. Kleinspehn & C. Paola), pp. 331–351. Springer-Verlag, New York, 444 pp.

CROSS, T. A. & HARBAUGH, J. W. (1990) Quantitative dynamic stratigraphy: a workshop, a philosphy, a methodology. In: *Quantitative Dynamic Stratigraphy* (Ed. by T. A. Cross), pp. 3–20. Prentice-Hall, Englewood Cliffs, NJ, 615 pp.

DICKINSON, W. R. (1988) Provenance and sediment dispersal in relation to paleotectonics and paleogeography of sedimentary basins. In: *New Perspectives in Basin Analysis* (Ed. by K. L. Kleinspehn & C. Paola), pp. 3–25. Springer-Verlag, New York, 444 pp.

FLEMINGS, P. B. & JORDAN, T. E. (1989) A synthetic stratigraphic model of foreland basin development. *J. geophys. Res.* **94**, 3851–3866.

GARDE, R. J., RANGA RAJU, K. G. & MEHTA, P. J. (1981) Bed level variation in aggrading alluvial streams. Int. Assoc. Hydr. Res. Congress, New Delhi, pp. 247–253.

GILL, M. A. (1983) Diffusion model for degrading channels. *J. Hydraul. Res.* **21**, 369–378.

HELLER, P. L., ANGEVINE, C. L., WINSLOW, N. S. & PAOLA, C. (1988) Two-phase stratigraphic model of foreland-basin sequences. *Geology* **16**, 501–504.

HELLER, P. L. & PAOLA, C. (1992) The large-scale dynamics of grain-size variation in alluvial basins, 2: Application to syntectonic conglomerate. *Basin Res.* **4**, 91–102.

HELLER, P. L., TABOR, R. W., O'NEIL, J. R., PEVEAR, D. R., SHAFIQUALLAH, M. & WINSLOW, N. S. (1992) Isotopic provenance of Paleogene sandstones from the accretionary core of the Olympic Mountains, Washington. *Bull. geol. Soc. Am.* **104**, 140–153.

JAIN, S. C. (1981) River bed aggradation due to overloading. *J. Hydraul. Div. Am. Soc. Civ. Engrs.* **107**, 120–124.

JARAMILLO, W. F. & JAIN, S. C. (1984) Aggradation and degradation of alluvial-channel beds. *J. Hydraul. Engrg.* **110**, 1072–1085.

JORDAN, T. E. & Flemings, P. B. (1990) From geodynamic models to basin fill – a stratigraphic perspective. In: *Quantitative Dynamic Stratigraphy* (Ed. by T. A. Cross), pp. 149–163. Prentice-Hall, Englewood Cliffs, NJ, 615 pp.

JORDAN, T. E., FLEMINGS, P. B. & BEER, J. A. (1988) Dating thrust activity by use of foreland basin strata. In: *New Perspectives in Basin Analysis* (Ed. by K. L. Kleinspehn & C. Paola), pp. 307–330. Springer-Verlag, New York, 444 pp.

KENYON, P. M. & TURCOTTE, D. L. (1985) Morphology of a delta prograding by bulk sediment transport. *Bull. geol. Soc. Am.* **96**, 1457–1465.

KRUMBEIN, W. C. (1941) The effects of abrasion on the size, shape, and roundness of rock fragments. *J. Geol.* **49**, 482–520.

KUENEN, P. H. (1956) Experimental abrasion of pebbles. 2. Rolling by current. *J. Geol.* **64**, 336–368.

KUSZNIR, N. & KARNER, G. (1985) Dependence on the flexural rigidity of the continental lithosphere on rheology and temperature. *Nature* **316**, 138–142.

LINDSAY, E. H., SMITH, G. A. & HAYNES, C. V. (1990) Late Cenozoic depositional history and geoarcheology, San Pedro Valley, Arizona. In: *Geologic Excursions through the Sonoran Desert Region, Arizona and Sonora* (Ed. by G. E. Gehrels & J. E. Spencer), pp. 9–19. Arizona Geological Survey, Tucson, Arizona.

MEYER-PETER, E. & MÜLLER, R. (1948) Formulas for bed-load transport. *2nd Mtg Int. Ass. Hydraulic Structures Research, Stockholm*, pp. 39–64.

MORETTI, I. & TURCOTTE, D. L. (1985) A model for erosion, sedimentation, and flexure with application to New Caledonia. *J. Geodyn.* **3**, 155–168.

PAOLA, C. (1988) Subsidence and gravel transport in alluvial basins. In: *New Perspectives in Basin Analysis* (Ed. by K. L. Kleinspehn & C. Paola), pp. 231–243. Springer-Verlag, New York, 444 pp.

PAOLA, C. (1990) A simple basin-filling model for coarse-grained alluvial systems. In: *Quantitative Dynamic Stratigraphy* (Ed. by T. A. Cross), pp. 363–374. Prentice-Hall, Englewood Cliffs, NJ, 615 pp.

PAOLA, C. & WILCOCK, P. (1989) Downstream fining in gravel bed rivers. *Eos, Trans. Am. geophys. Un.* **70**, 852.

PARKER, G. (1978) Self-formed straight rivers with equilibrium banks and mobile bed. Part 2. The gravel river. *J. fluid Mech.* **89**, 127–146.

PARKER, G. (1991a) Selective sorting and abrasion of river gravel, I: theory. *J. Hydraul. Engrg.* **117**, 131–149.

PARKER, G. (1991b) Selective sorting and abrasion of river gravel, II: applications. *J. Hydraul. Engrg.* **117**, 150–171.

PARKER, G. (in press) Some random notes on grain sorting. *I. A. H. R. Grain Sorting Seminar, Ascona, Italy, October 1991.*

PLUMLEY, W. J. (1948) Black Hills terrace gravels: a study in sediment transport. *J. Geol.* **56**, 526–577.

PRESS, W. H., FLANNERY, B. P., TUEKOLSKY, S. A. & VETTERLING, W. T. (1986) *Numerical Recipes.* Cambridge University Press, Cambridge, UK, 795 pp.

RIBBERINK, J. S. & VAN DER SANDE, J. T. M. (1985) Aggradation in rivers due to overloading – analytical approaches. *J. Hydraul. Res.* **23**, 273–284.

RUST, B. R. & KOSTER, E. H. (1984) Coarse alluvial deposits. In: *Facies Models, 2nd edn* (Ed. R. G. Walker). *Geosci. Canada* **1**, 53–69.

SCHUMM, S. A. & STEVENS, M. A. (1973) Abrasion in place: a mechanism for rounding and size reduction of coarse sediments in rivers. *Geology* **1**, 37–40.

SHAW, J. & KELLERHALS, R. (1982) *The Composition of Recent Alluvial Gravels in Alberta River Beds. Bull. Alberta Res. Council* **41**, 151 pp.

SMITH, G. A. & BATTUELLO, P. A. (1990) Sedimentation pattern of a rift-filling unit, Tesuque Formation (Miocene), Espanola Basin, Rio Grande Rift, New Mexico – Discussion. *J. sedim. Petrol.* **60**, 175–177.

SONI, J. P. (1981) Unsteady sediment transport law and prediction of aggradation parameters. *Water Resour. Res.* **17**, 33–40.

ZHANG, H. & KAHAWITA, R. (1987) Nonlinear model for aggradation in alluvial channels. *J. Hydraul. Engrg.* **113**, 353–369.